Infrared Detection Using Plasmonically Enhanced Thermomechanically Actuated Nanowire Arrays

Qiancheng Zhao, Parinaz Sadri-Moshkenani, Mohammad Wahiduzzaman Khan, Rasul Torun, Imam-Uz Zaman, and Ozdal Boyraz

Department of Electrical Engineering and Computer Science, University of California, Irvine, California, 92697, USA
oboyraz@uci.edu

Abstract: A plasmo-thermomechanical IR detector based on suspended bilayer nanowire array is demonstrated. The detector exhibits an absorption coefficient of 0.0494. The maximum difference in S_{21} between the radiation *on* and *off* states is 0.013 with a radiation intensity of 0.1 mW/μm^2.
OCIS codes: (040.3060) Infrared; (040.1880) Detection; (310.6628) Nanostructures.

1. Introduction

The fundamental concept behind the infrared detection is the transduction mechanism that enables the energy conversion from the electromagnetic domain to others. Most of the infrared detector may be classified as either quantum or thermal detectors [1]. Thermoplasmonics, which takes advantage of photo thermal effects caused by the light absorption in the resonant metallic nanoantennas, has drawn tremendous attention to convert energy in electromagnetic domain into thermal domain in the applications of energy harvesting [2]. The photo thermal effects can be detected by the thermal detectors, i.e., thermally actuated bilayer cantilevers [3] or membranes [4].

Inspired by our recent achievement of the optical leaky wave antennas (OLWAs) [5], in which the perturbation wire arrays can not only generate the radiation patterns but also attenuate the transmission power in the waveguide, here we propose a novel plasmo-thermomechanical detector for the infrared radiation. The radiation is transduced into heat by the fishbone antenna unit cells that exhibit an absorption coefficient of 0.0494 at the wavelength of 785 nm. These antennas are connected by the bilayer nanobeams that are composed of 30 nm gold (Au) and 20 nm nickel (Ni) layers. The center of the nanobeam will be elevated 3.36 nm due to the mismatch of the thermal expansion coefficients of the two materials given a normal incident power density of 0.1 mW/μm^2, which alternates the output power from the waveguide. The detector shows a maximum change in S_{21} to be 0.013 in our theoretical design. We also show that the approach is scalable and can be extend to the mid-IR regime such as 4.3 μm.

2. Device Model and Thermomechanical Actuator

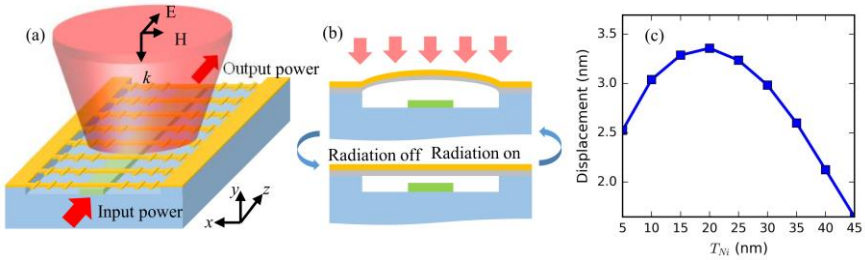

Fig. 1 (a) The concept figure of the radiation detector. (b) The cross section view of the radiation *on* and *off* states. (c) The displacement in the center of the nanowire as a function of the bottom Ni layer thickness T_{Ni}.

As demonstrated in Fig. 1(a), the thermoplasmonic detector is composed of a silicon nitride (Si_3N_4) waveguide and an array of bilayer fishbone nanowires that are suspended above the waveguide to create weakly coupled leaky wave antennas. When the infrared energy is transduced by the fishbone antennas to the nanowires, the temperature variation will thermally actuate the nanowires, and thus changes the gap between the nanowires and the waveguide top surface, as illustrated in Fig. 1(b). The deformation of the nanowires can modulate the evanescent field from the waveguide, and hence changes the transmitted and radiated power. To illustrate the concept, we select the waveguide with 1.5 μm × 0.3 μm dimensions to guarantee the single TE mode (electric field oscillating along the *x* axis) operation at the wavelength of 1550 nm. The gap between the nanowire and the waveguide is set to be 50 nm in our design, and it can be achieved by etching the silicon dioxide (SiO_2) sacrifice layer with hydrogen fluoride (HF) vapor. For the sake of fabrication compatibility, Au and Ni are used to build the nanobridge due to their chemical resistance to HF. Since Au has a larger thermal expansion coefficient (14.2×10^{-6} /K) than Ni (13.4×10^{-6} /K), the top and bottom layers should be Au and Ni, respectively, so that the nanowire will bend upward to avoid collapsing and sticking to the waveguide surface. The total metal layer thickness is set to be 50 nm. Simulation results, shown in Fig. 1(c), indicate that a 20 nm Ni layer at the bottom can yield the largest displacement on a 11.16 μm long nanobeam. The simulation was done by assigning a temperature profile that will be elaborated later (Fig.

3(a)). The heat transfer coefficient on the wire surface is assigned to be 5 W/(m^2·K) to mimic the air cooling, and the ambient temperature is set to be 293.15 K in the simulations.

3. Plasmonic Fishbone Nanostrip Antenna

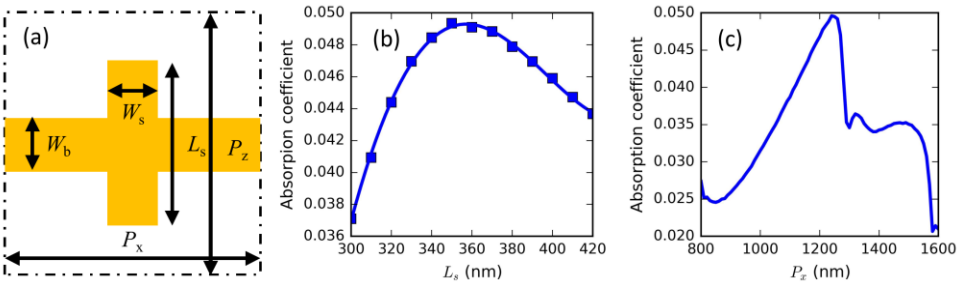

Fig. 2 (a) The schematic of the fishbone antenna unit cell. (b) The absorption power as a function of the antenna length L_s. (c) The absorption coefficient as a function of cell period in the *x* direction P_x.

Fishbone nanostrip antennas are employed to absorb the infrared radiation at 785 nm. For this wavelength, the relative permittivities of the Au and Ni are -21.01 - *j*1.69 and -12.95 - *j*22.42, respectively. In the simulations, the fishbone antenna, surrounded by air, is assumed to be suspended 350 nm above a SiO_2 substrate for simplicity. The electric field is polarized along the *z* direction. The nanostrip width W_s and the nanobeam width W_b in Fig. 2(a) are set to be equal to 100 nm. The resonant length of the antennas, L_s, is optimized to 350 nm to achieve the peak absorption coefficient of 0.0494 as depicted in Fig. 2(b). To increase the total absorbed energy, multiple antennas will be connected by a single nanobeam. The period of the fishbone antenna unit cell in the *z* direction is set to be 1 μm and is constrained by the design of nanowire grating. The period in the *x* direction is tuned to find the optimum spacing between the antennas in Fig. 2(c). A period of 1.24 μm in the *x* direction can yield the highest absorption coefficient. Assume the nanowire is 11.16 μm long, 6 nanostrip antennas can be arranged on one nanowire, leaving a 3.72 μm wide space in the center of the nanobeam for the waveguide underneath. Under 0.1 mW/μm^2 radiation density, the temperature in the center of the nanowire can reach 331.8 K as shown in Fig. 3(a). By fitting the temperature profile using a piecewise function approximately and feeding the function into the thermomechanical simulation model, the maximum displacement is found to be 3.36 nm as shown in Fig. 3(b).

4. Wire Array Design

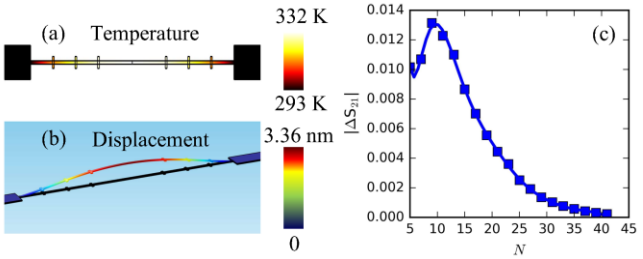

Fig. 3 (a) The temperature profile in the symmetric plane (*x*-*y* plane) of the nanowire. (b) The perspective view of the displacement as a result of the temperature increment in (a). (c) The difference in S_{21} caused by the nanowire displacement as a function of the nanowire number.

Instead of converting optical energy into charged carriers directly we use a detector model that is based on the OLWA, where the nanowire array can produce directive emission. We show that the displacement of the nanowire modulates the emission pattern of a wave propagating in the waveguide. To achieve broadside emission, the period of the wires is optimized to be 1 μm, yielding an emission angle of 89.5° at 1550nm. The investigation of the displacement effects on the emission pattern will be presented in a future research. In this study, we focus on the waveguide output power, especially the difference of the S_{21} between the radiation *on* and *off* states is of interest. The number of the wires *N* can affect the S_{21} difference. Too few wires will cause limited modulation strength, while too many wires can attenuate the output power severely. Assuming the gap between the wire and the waveguide is 50 nm and a displacement of 3.36 nm, we find that when *N* equals 10, the difference in S_{21} gets the maximum value of 0.013 as shown in Fig. 3(c). It is worth noting that the research methodology can be extended to detect visible or mid-IR spectrum. Findings on the simultaneous detection of 785 nm and 4.3 μm radiation will also be presented.

This work was supported by the National Science Foundation under NSF Award # ECCS-1449397.

References

1. T. W. Kenny, et.al, "Novel infrared detector based on a tunneling displacement transducer," Appl. Phys. Lett. **59**, 1820–1822 (1991).
2. J. Agustí Batlle and G. Abadal Berini, *Nonlinear Micro/nano-Optomechanical Oscillators for Energy Transduction from IR Sources* (Universitat Autònoma de Barcelona, 2015).
3. M. Toda, et.al, "Evaluation of bimaterial cantilever beam for heat sensing at atmospheric pressure," Rev. Sci. Instrum. **81**, 55104 (2010).
4. F. Yi, et.al, "Plasmonically Enhanced Thermomechanical Detection of Infrared Radiation," Nano Lett. 130320090705008 (2013).
5. Q. Zhao, et.al, "Experimental Demonstration of Directive Si3N4 Optical Leaky Wave Antennas With Semiconductor Perturbations," J. Light. Technol. **34**, 4864–4871 (2016).